Int. J. Electrochem. Sci., 13 **(2018)** 498 – 513, doi: 10.20964/2018.01.35

International Journal of
ELECTROCHEMICAL
SCIENCE
www.electrochemsci.org

Electrochemical Chloride Extraction and Inhibitor Injection in Salt-Contaminated Repair Mortar

Jing Gong[1], *Zhang Shen*[1], *Yangyang Tong*[1], *Zhipeng Li*[1], *Xianming Shi*[2,*]

[1] School of Civil Engineering & Architecture, Wuhan Polytechnic University, 430023, Wuhan, China
[2] Laboratory of Corrosion Science & Electrochemical Engineering, Department of Civil and Environmental Engineering, P. O. Box 642910, Washington State University; Pullman, WA 99164-2910, USA
[*]E-mail: xianming.shi@wsu.edu

Received: 27 August 2017 / *Accepted:* 15 October 2017 / *Online Published:* 1 December 2017

Repair mortar is commonly used to rehabilitate reinforced concrete structures or components that exhibit a relatively high level of distresses. Yet, the repair mortar can be contaminated by salt from its service environment. This work employs a two-dimensional finite element model to investigate the non-stationary transport behavior of ionic species in salt-contaminated and water-saturated repair mortar under an externally applied electric field. The model was experimentally validated and then utilized to evaluate the effectiveness of electrochemical chloride extraction (ECE) with or without electrical injection of corrosion inhibitor (EICI). In the case study, both the ECE alone and the simultaneous ECE+EICI treatment was found effective in decontaminating the zone in front of the steel rebar. In both techniques, the magnitude of current density had a significant effect on removing chloride out of the mortar and increasing the pH of the pore solution near the rebar, whereas the treatment time did not have a significant effect under some scenarios. The injection of the organic corrosion inhibitor significantly slowed down the removal of chloride. Changes in the ionic distribution in the mortar were generally beneficial in reducing the corrosion risk of the steel rebar and thus extending the service life of the repair mortar.

Keywords: Finite Element Modeling; electrochemical chloride extraction (ECE); electrical injection of corrosion inhibitor (EICI); Rebar Corrosion; Repair Mortar

1. INTRODUCTION

Excessive accumulation of some species from the environment can be harmful to the service life of concrete structures [1, 2], such as buildings and bridges. In addition to freeze/thaw damage, the ingress of and attack by chlorides, carbon dioxide, and sulfates have been reported as the major mechanisms that deteriorate reinforced concrete and lead to a subsequent reduction in the strength,

performance, and aesthetics of structures [3-8]. The gradual ingress of atmospheric carbon dioxide into the concrete (carbonation) can reduce the pH of the concrete pore solution and degrade the concrete matrix [4, 5]. Chlorides anions, often originated from marine environments or winter road maintenance operations, can initiate the rebar corrosion once their concentration exceeds a threshold level [9-11] and lead to premature deterioration of reinforced or prestressed concrete.

The durability and serviceability of concrete (or mortar) and the embedded rebar can be improved by limiting the amount of undesirable species or incorporating beneficial species in concrete [12, 13]. As such, engineers have developed various approaches to enforce the transport of species under applied physical fields. Such enforced transport approaches include both extraction of deleterious species and injection of beneficial species. For instance, electrochemical chloride extraction (ECE) has proven to be an effective chloride removal approach to treating salt-contaminated concretes [14-16]. In ECE, chloride anions are electrically driven towards a temporary external anode and potentially out of concrete while generating beneficial hydroxyl ions at the reinforcing steel [17]. In ECE, an electric field of 1~5 A/m^2 of steel surface is usually applied to a concrete component to minimize possible damage to the steel-concrete bond or the concrete matrix. Liu and Shi [18] conducted a numerical investigation to examine the effect of various factors (external current density, treatment time, initial chloride content, rebar position, coarse aggregates, and cracks) on the efficiency of removing chlorides from heterogeneous concrete materials. Yodsudjai and Saelim [19] conducted a laboratory investigation of ECE on concrete specimens with a water-to-cement ratio of 0.45 and found that "76% of chloride content could be removed … at 2 cm depth from concrete surface", after a 28-day, 15-Volt treatment using saturated lime solution as the external electrolyte. Polder et al. [20] reported that the efficiency of ECE treatment was higher with the use of saturated lime solution instead of sodium carbonate as electrolyte. Cañón et al. [21] developed a sprayed conductive cement paste as the external anode for ECE, which removes the need for a continuous dampening system during ECE. The use of an external electric field has other applications including the realkalization of carbonated concrete [22, 23], the mitigation of alkali-silica reaction (ASR) by electrical injection of lithium ions into concrete [24], the closure of cracks by electrical injection of zinc cations into concrete followed by formation of electrodeposits [25], etc.

Electrical injection of corrosion inhibitor (EICI) emerged recently as a promising solution to rebar corrosion in concrete structures [26-30]. Pan et al. [27] conducted a laboratory investigation to identify available organic cation-based inhibitors for EICI and reported a subsequent numerical investigation to examine the effect of various factors (inhibitor type, current density, and treatment time) on the efficiency of EICI into concrete. Liu and Shi [28] presented a comprehensive review on the state of knowledge about ECE and EICI, which covered both laboratory and numerical studies. Sánchez and Alonso [29] reported that the injection of nitrite (an anion-based inhibitor) during ECE was facilitated by using a non-traditional configuration featuring an external cathode (instead of anode) to the rebar.

Repair mortar is commonly used to rehabilitate reinforced concrete structures or components that exhibit a relatively high level of distresses. The mortar is often applied to the bridge or building structure once the damaged concrete is removed and corroded rebar is cleaned [12, 30]. Yet, this repair mortar can be contaminated by salt from its service environment. Mortar as a composite material

includes fine aggregates and cement hydration products that may physically or chemically bind ionic species. Such binding removes chloride anions from the pore solution, and slows down the rate of penetration [31-33]. It is generally believed that only the free chlorides can promote pitting corrosion, while the bound chlorides such as those adsorbed on C-S-H or chemically bound with mortar C_3A or C_4AF phases (e.g., Friedel's salt, $3CaO{\cdot}Al_2O_3{\cdot}CaCl_2{\cdot}10H_2O$) do not. However, a more recent study suggests that bound chlorides also play a role in corrosion initiation once the pH drops to values below 12 [34].

Experimental studies have found an ECE or EICI treatment at current density of 1 A/m^2 and 5 A/m^2 for as short as four weeks to effectively decrease the corrosion rate of the embedded steel rebar in salt-contaminated repair mortar of one 25-mm cover [35, 36]. It is thus desirable to employ numerical simulation to shed more light on how the electrochemical treatments affect the distribution of ionic species in the mortar, without significantly increasing the laboratory work needed. In this context, this work employs a two-dimensional (2D) numerical model to describe the transport of co-existent species in salt-contaminated repair mortar under an externally applied electric field (ECE and EICI).

2. METHODOLOGY

2.1. Laboratory Measurement of Input Parameters of the Model

A commercially available chemical, tetrabutylammonium bromide (TBA-B) was used as the corrosion inhibitor in this study, with its organic cation (TBA^+) serving to inhibit the chloride-induced corrosion of carbon steel once adsorbed onto the metallic substrate. The inhibition efficiency of this inhibitor has been previously confirmed by Pan et al. [27]. In determining the evolution of chloride and inhibitors in mortar, other species including mainly the sodium (Na^+), potassium (K^+), and hydroxyl (OH^-) ions are considered in the numerical investigation.

The numerical investigation needed the apparent diffusion coefficient (D_{app}) for each of the five ionic species included in the model. The D_{app} values of chloride and TBA-B are highly dependent on the materials properties of the repair mortar, e.g., chemistry of cement hydration products and microstructure (porosity, tortuosity, and constrictivity) of mortar matrix. In this study, the 2″ by 4″ (5.1 cm in diameter by 10.2 cm in length) mortar specimens used Type I/II cement and used only sand with a diameter ranging from 0.85 mm to 2.0 mm. The cement: water: sand ratio by weight was 1:0.5:3.5 for the mortar specimens. The air content in fresh mortar was measured to be 2.1%, following the ASTM C185 standard test method. The mortar specimens were cured in a wet chamber for 28 days. Subsequently, the D_{app} value of TBA-B in the hardened mortar was measured in the laboratory using a modified electromigration method developed by Pan et al. [27], respectively. The electromigration test maintained an applied current density of 6 A/m^2 of steel surface and employed 1″ (2.54 cm) thick disc samples cut from the center of the mortar specimens. The TBA-B concentration of the destination solution was monitored up to 28 days on a daily basis. The D_{app} was calculated based on a method detailed elsewhere [33] and the results averaged from triplicate disc samples led to a D_{app} value of 1.2×10^{-11} m^2/s for TBA-B. Chloride diffusivity in salt-

contaminated mortar likely deviates from that in non-contaminated mortar; as such, sodium chloride was admixed into the fresh mortar at 1:100 by weight of cement and an average D_{app} value of 4.06×10^{-11} m^2/s was obtained for the Cl^- diffusivity, following the same method used to measure D_{app} of TBA-B. The D_{app} values of Na^+, K^+, and OH^-, however, are relatively less sensitive to the mortar constituents [37] and were therefore obtained from literature.

The α and β values characteristic of the Langmuir binding isotherm of chloride anions [32] were determined by measuring the chloride concentrations inside the mortar discs subsequent to the electromigration tests. The mortar discs were cut into three thinner slices with equal thickness. The samples were ground and then boiled in water or nitric acid, followed by chemical titration, in order to determine the free (i.e., water soluble) and total (acid soluble) chloride concentrations, respectively [38]. The α and β values characteristic of the binding of TBA-B were also determined following the same sample preparation method, except that the inhibitor concentration was determined using ultraviolet-visible (UV-vis) spectroscopy as detailed elsewhere [39]. The inhibitor concentration in a given solution is proportional to the signal strength of a characteristic peak on the inhibitor's UV-vis spectrum.

2.2. Description of the Model

The 2D model aims to capture the main features of ionic transport in mortar by considering the integration of multiple ionic species, the ionic binding with cement hydration products, and the microstructural influence of mortar matrix. The model was coded and compiled as a finite element method (FEM) program based on the Galerkin method, a commonly used weighted residual method [40, 41]. An algorithm involving a double-loop iteration was developed to solve the non-linear equations [42]. The algorithms for solving the non-linear systems were coded and compiled into an executable program using the Matlab™ and COMSOL Multiphysics™ software packages. A stability parameter of 0.5 was used for the time-dependent solver. The forward calculation and other details of the model are provided in our previous work [18]. The FEM program was then used in this study to predict the concentration evolution of chloride and inhibitor in the domain of repair mortar. Note that this model does not consider any change in the diffusivity coefficients or binding parameters due to the electrochemical treatments [36].

The establishment of the 2D model stems from the mass balance equation of multiple ionic species in an electrolyte, considering the mass transport flux of the free ions (J_i) through a pre-defined finite domain, the binding of TBA^+ and Cl^- by the mortar, the production of OH^- ions at the rebar surface during the electrochemical treatment, as well as a set of boundary conditions for the concentration fields and electric field. In the repair mortar, there are three main mechanisms that affect the flux of various species, i.e., natural diffusion, electric migration, and transport along with the pore solution. For the water-saturated mortar without any externally applied pressure, species transport through the last mechanism is negligible. For ions with high concentrations, Li and Page [43] illustrated the need to incorporate the ion activity coefficients into the modeling of ECE. As such, the "effective concentration" calculations in this work were based on the mathematical model for

calculating the chemical activity coefficients of ions presented by Samson et al. [44]. The influence of solution non-ideality on ionic fluxes was found negligible when the electrolyte was subjected to an externally applied electric field that was much stronger than the internally induced electric fields created by the transport of species carrying opposite charges. In other words, the transport of species in the mortar pore solution was controlled by the divergence of the gradients of concentration and applied electric potential, as shown in Eqn. 1.

$$\frac{\partial C(i)}{\partial t} = \nabla \cdot D(i)(\nabla C(i)) + \nabla \cdot \left[Z(i)\frac{D(i)F}{RT}C(i)(\nabla \phi)\right], \mathrm{i} = 1, 2, 3, \ldots \mathrm{m} \quad (1)$$

In Eqn. 1, *C(i)*, *D(i)*, *z(i)* and *t* denotes the free concentration, diffusion coefficient, and valence number of species *i* and time, respectively, whereas *F*, *R*, and *T* denotes the Faraday constant, ideal gas constant, and absolute temperature, respectively. *ø* is the potential of the externally applied electric field.

A few assumptions were made regarding the boundary conditions. The steel rebar (cathode) during the electrochemical treatment was assumed to be free of active corrosion and so was the external anode. The half-reaction occurring at the cathode is assumed to be the production of hydroxyl ions via reduction of water and oxygen, which features a flux proportional to the externally applied current density. The electric potential on the anode is set to zero and all the species other than hydroxyl ions have zero flux on the cathode.

The model considers the contribution of all the main ionic species in the pore solution (TBA^+, Na^+, K^+, OH^-, and Cl^-) to the total electric current flux under the externally applied electrical field. The electro-neutrality condition was maintained to account for the interactions between negatively and positively charged ions, and the transference numbers of the key ionic species were incorporated into the model as well [45]. Pereira et al. [46] suggested a Langmuir isotherm (Eqn. 2) for describing ionic binding to cement hydration products; as such, the binding of TBA^+ and Cl^- was assumed to follow Langmuir isotherm

$$C(bi) = \frac{\alpha \times C(fi)}{1 + \beta \times C(fi)} \quad (2)$$

In Eqn. 2, *C(bi)* and *C(fi)* denote the bound and free concentration of species *i*, respectively, whereas α and β are two interrelated parameters defined by the properties of the mortar and the species type.

3. RESULTS

3.1. Validation of the FEM Model

The chloride or inhibitor concentration profiles from water-saturated mortar discs of 45-mm cover over the steel rebar were utilized to validate the developed FEM model. The input parameters for the FEM model are summarized in Table 1 and the water/cement ratio of the mortar mixtures was 0.50 and the mixing water contained NaCl at 1% by weight of cement. Mortars with admixed chloride may differ significantly from mortars with their counterparts with chloride ingress from the service environment. Yet, the admixed NaCl compromises the physicochemical characteristics of hydrated mortar [13]; as such, in this case study, this simplistic approach was adopted to simulate a repair

mortar compromised by the ingress of external chlorides. For one batch of samples, after a 14-day, 1 A/m^2 of ECE treatment, the free chloride concentration (averaged across the cross-section) was measured at two depths along the axis of each mortar disc (5-10 mm and 15-20 mm), following the titration method [38].

Table 1. Input Parameters for the FEM model

Parameters	Physical Meaning	Magnitude
I_0	current density	in A/m^2 of steel rebar surface
F	Faraday's constant	9.64846×10^4 C/mol
R	Ideal gas constant	8.3143 J/(mol·K)
T	Absolute temperature	298.15 K (25 °C)
$\alpha_{(Cl)}$	Langmuir Isotherm parameter for Cl^-	1.6×10^{-4} m^3/mol
$\beta_{(Cl)}$	Langmuir Isotherm parameter for Cl^-	4.05×10^{-3} m^3/mol
$\alpha_{(TBA)}$	Langmuir Isotherm parameter for TBA-B	1.0×10^{-4} m^3/mol
$\beta_{(TBA)}$	Langmuir Isotherm parameter for TBA-B	2.31×10^{-3} m^3/mol

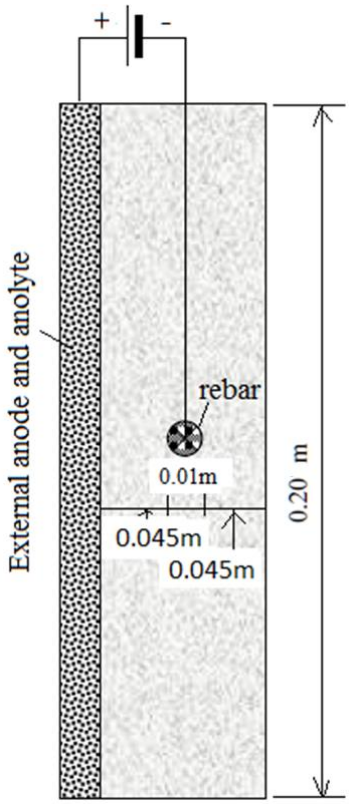

Figure 1. Schematic Illustration of the 2D Mortar Domain to Be Analyzed

For another batch of samples, after a 28-day, 5 A/m^2 of 500 mM TBA-B inhibitor electromigration (simultaneous ECE+EICI), the free inhibitor concentration (along with free chloride concentration) was measured at two depths along the axis of each mortar disc (5-10 mm and 15-20

mm), following the UV-vis method [39]. These measured free chloride and inhibitor concentrations were found to agree reasonably well with the predicted average concentrations at the two given depths (within ±12.5%). This validated the FEM model, as the differences can be partly attributable to experimental variability. The validated model was then employed to evaluate the effectiveness of the coupled ECE and EICI as a new corrosion protection technique for the rebar embedded in mortar, as detailed in the next sections. It is cautioned that the model validation was based on a limited number of case studies whereas the model simulation was extended to a wide variety of operating conditions.

3.2. Domain and Input Parameters of FEM Analyses

The FEM analyses were conducted using a simulated mortar specimen, a 0.20 m × 0.20 m (8″×8″) square-shaped prism with a thickness of 0.10 m (3.94″) and the same mix design as the ones used for laboratory measurement of D_{app} values of chloride and TBA-B. A commonly used steel rebar with the diameter of 0.01 m (0.4″) passes through the centroid of the length-height cross-section. The geometry of the cross-section, which is also the mortar domain to be modeled, is given in Figure 1. Note that the thickness of repair mortar is assumed to be 0.045 m (1.77″) in this case, while in practice the repair mortar could be up to 0.076 m (3″) thick. The repair mortar modeled features a water/cement ratio of 0.5 (and thus the relatively high D_{app} values), while in practice the repair mortar could feature a water/binder of 0.4 or lower. In other words, the simulated mortar represents a worst-case scenario where the protective thickness and resistance to permeation of the repair mortar had been compromised. Furthermore, the mortar is assumed to be a homogenous matrix with the given diffusion properties, without simulation of the specific porosity and tortuosity.

The input parameters for the FEM analyses are summarized in Table 1. The current density I_0 was applied directly as boundary condition, and magnitudes of 1, 3, 5 A/m^2 of steel rebar surface were used, respectively. Table 2 lists the chemical valence, ionic diffusion coefficients as well as the boundary and initial conditions of the various ionic species to be studied in the FEM model. The left-hand boundary in Figure 1 is next to the anolyte solution which maintains a body of running water to keep all the species at a constant concentration. Accordingly, the boundary conditions on the left-hand boundary are Dirichlet boundary conditions [47] for all the five species, i.e., $[Ci] = [Ci]_{anolyte}$ as given in Table 2. The electrical potential on the left-hand boundary was set at zero, i.e., $ø = 0$ as the reference potential. On the right-hand, top and bottom boundaries, the Neumann boundary conditions [48] were applied for all the species, i.e., $J_i = 0$ and $I_x = I_y = 0$. On the internal boundary (rebar surface), the Dirichlet boundary conditions were applied for the species Cl^-, Na^+, K^+, and TBA-B; and the Neumann boundary conditions were applied for the variable $ø$, i.e., $I = I_0$. The Neumann boundary conditions were also applied for the OH^- on the internal boundary based on the assumption that externally supplied current flux is maintained by the production of a constant hydroxyl flux on the rebar surface, i.e., $J_{OH^-} = I_0/FzOH^-$.

Table 2. Chemical Property and Initial Concentrations of the Ionic Species

Parameters	Cl^-	OH^-	Na^+	K^+	TBA-B
z_i	-1	-1	+1	+1	+1
D_i (m^2/s)	4.06×10^{-11}	1.01×10^{-10}	2.66×10^{-11}	3.92×10^{-11}	1.20×10^{-11}
*$[C_i]$mortar (mM)	513	100	513	100	0
$[C_i]$anolyte (mM)	0	400	400	0	200, 500

* $[C_i]$mortar is the free chloride concentration in the pore solution of the repair mortar. All the ionic concentrations in Table 2 are initial values as they change during the electrochemical treatment.

3.3. Results of FEM Analyses

The occurrence of rebar corrosion in mortar relies heavily on the relative concentrations of aggressive chloride and protective hydroxyl ions at the rebar surface [27]. Chloride anions can act as a catalyst in the anodic reaction of corrosion process once they penetrate the mortar cover and exceed a threshold level to disrupt the passive film on the rebar surface [10]. While the chloride threshold has been expressed as the free chloride concentration or total chloride concentration, the chloride-to-hydroxyl concentration ($[Cl^-]/[OH^-]$) ratio is a more reliable indicator, as the competition of aggressive Cl^- and inhibitive OH^- governs the pitting/repassivation of steel.

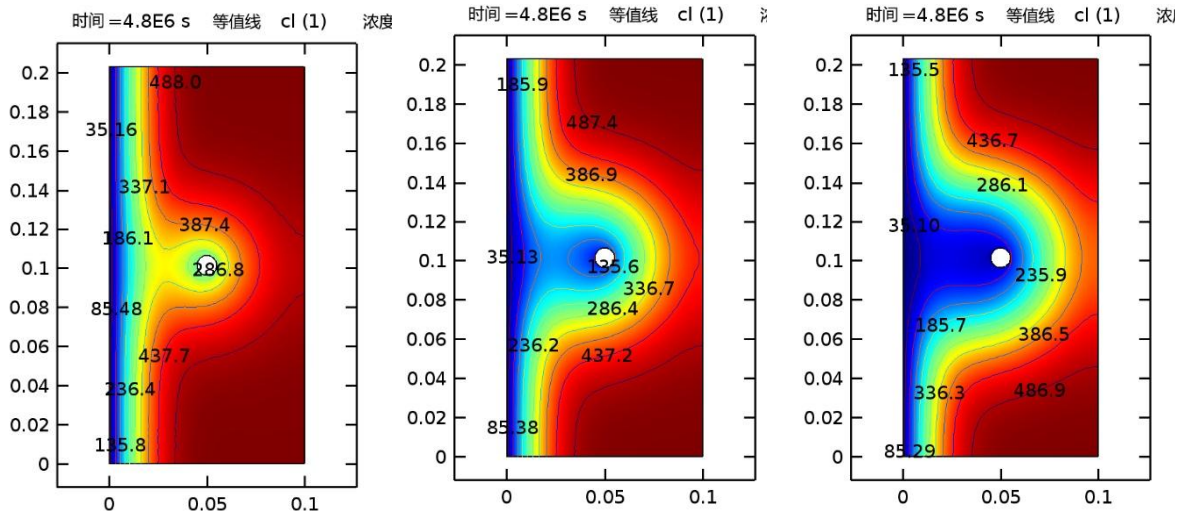

(a) Treatment at 1 A/m^2 (b) Treatment at 3 A/m^2 (c) Treatment at 5 A/m^2

Figure 2. Profiles of Free Cl^- concentration (mM) after the 8-Week ECE Treatment, As a Function of Current Density

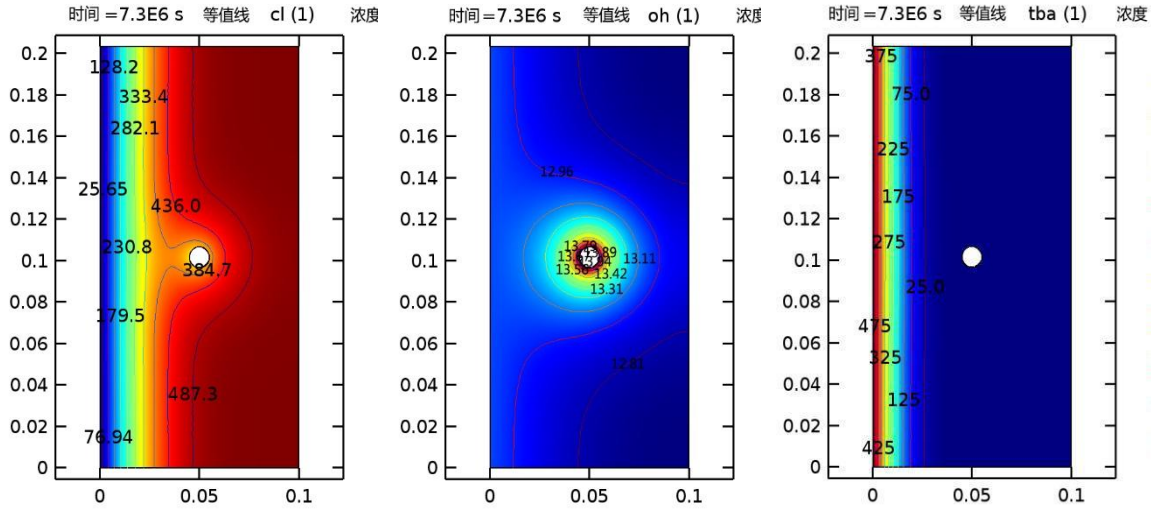

(a) Treatment at 1 A/m^2

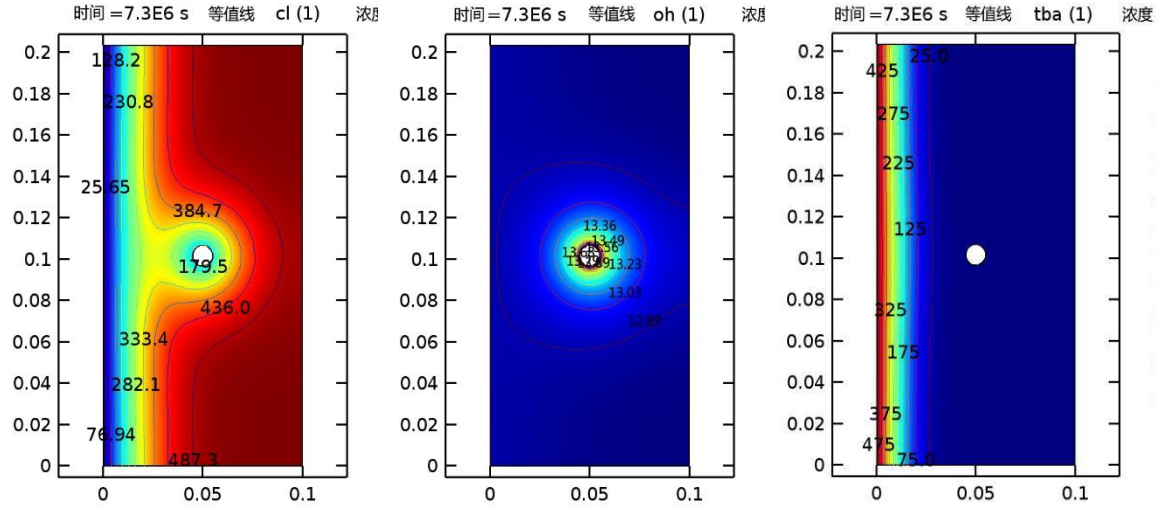

(b) Treatment at 3 A/m^2

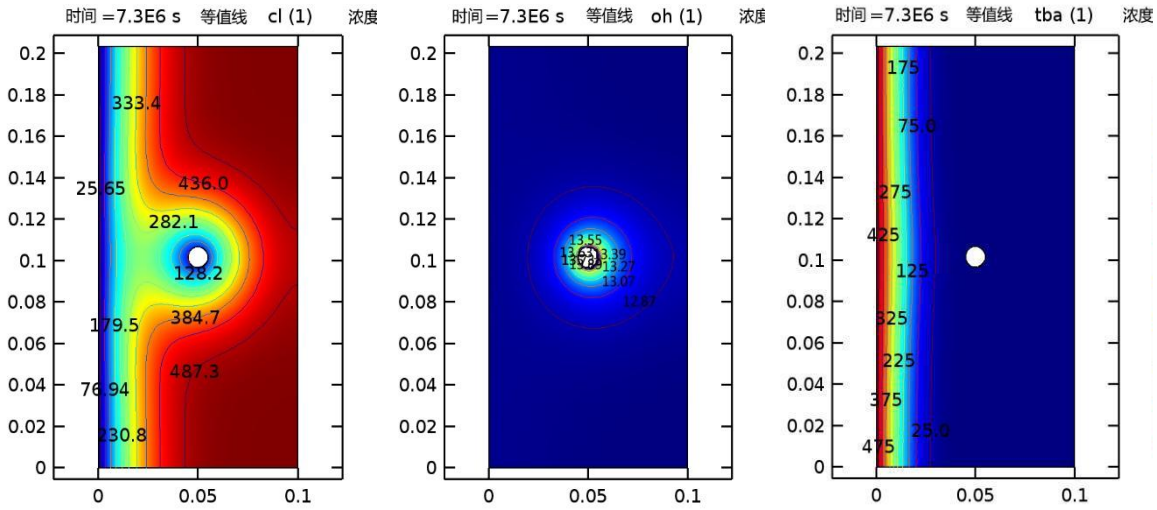

(c) Treatment at 5 A/m^2

Figure 3. Profiles of Free Cl^- (Left) and Free TBA^+ (Right) concentrations (mM) and pH Levels (Middle) after the 12-Week, 500 mM TBA-B Treatment, As a Function of Current Density

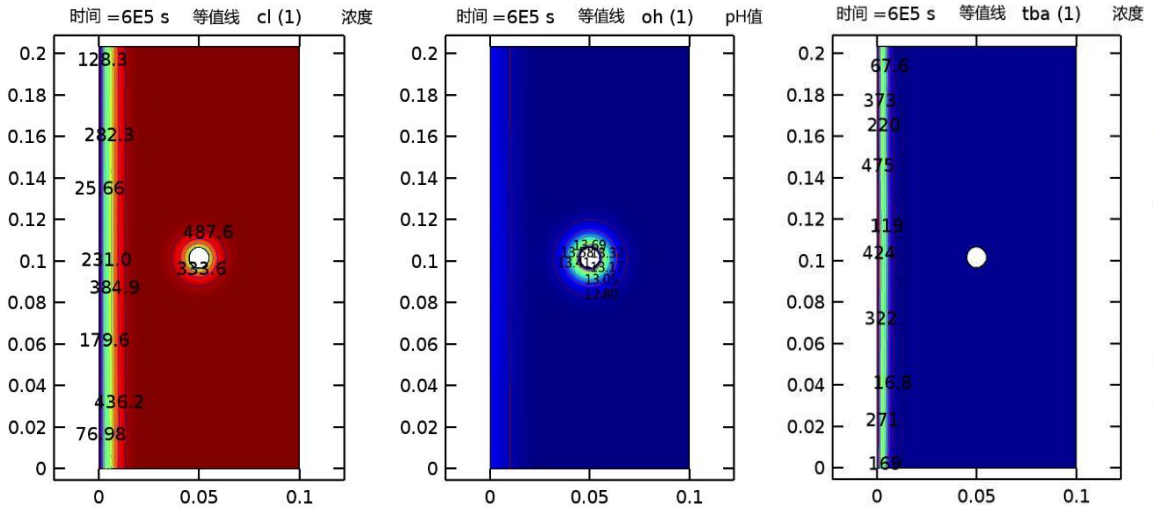

(a) Treatment of One Week

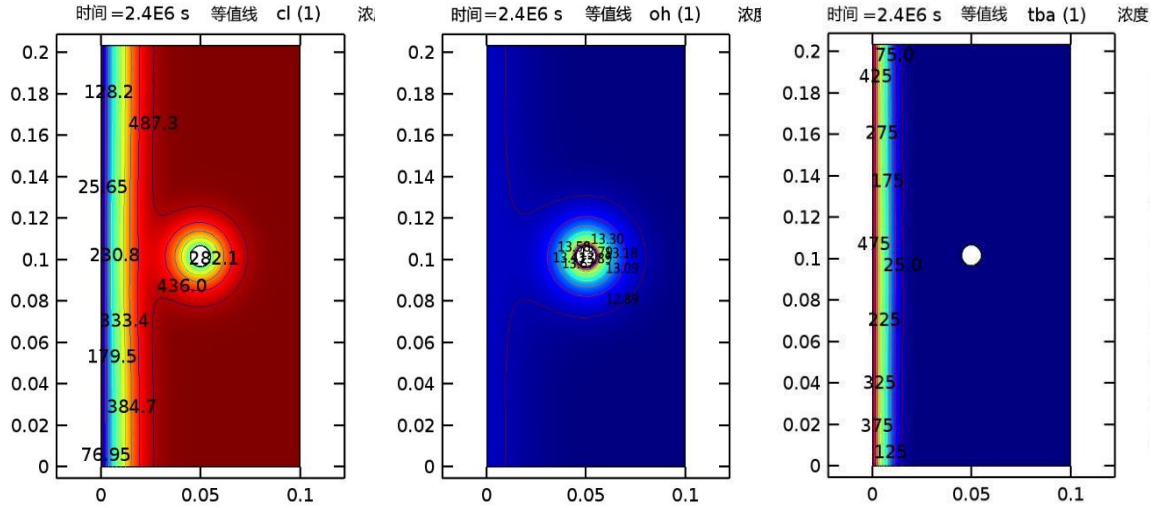

(b)Treatment of Four Weeks

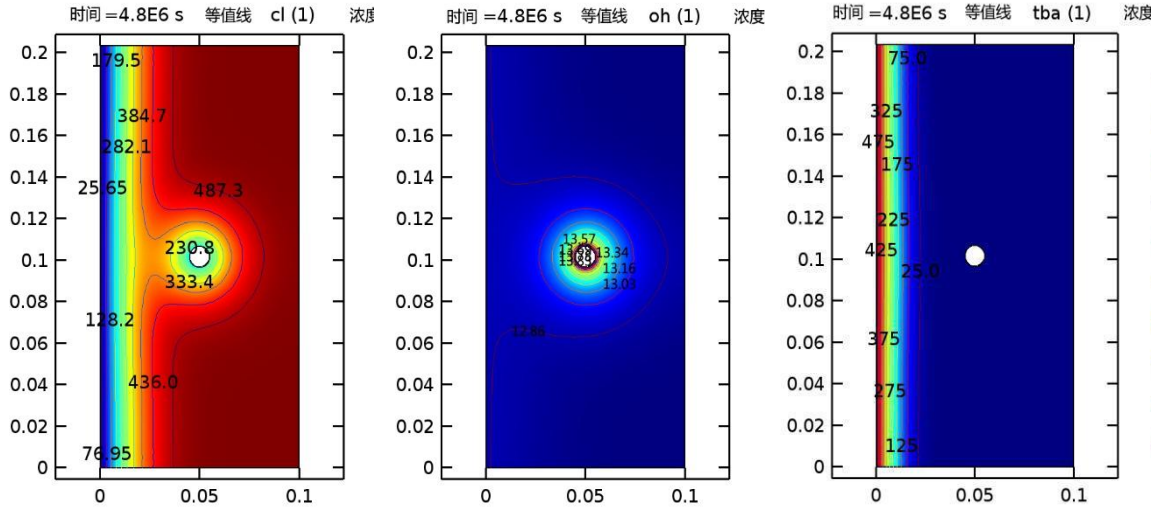

(c) Treatment of Eight Weeks

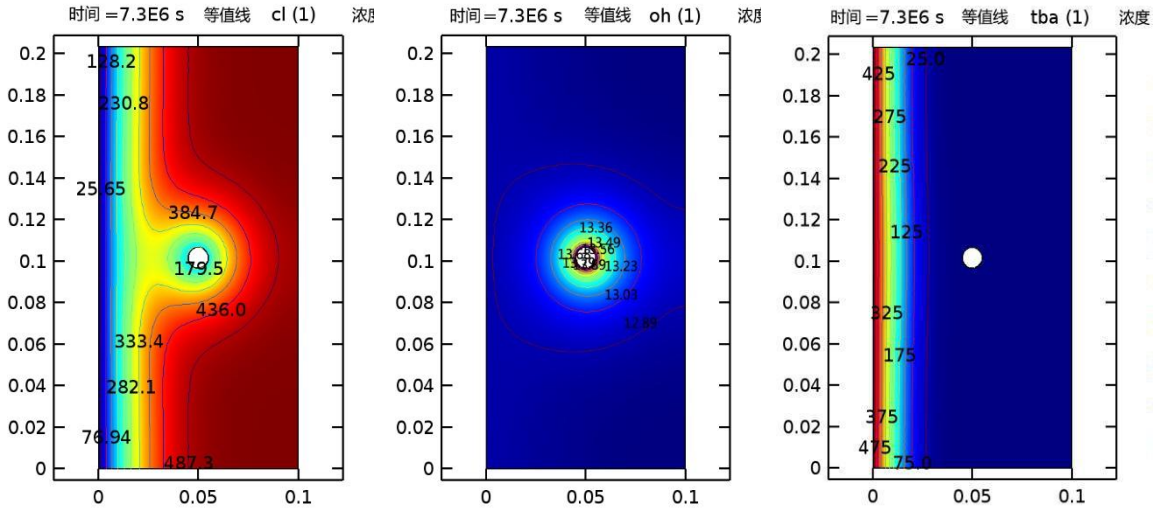

(d) Treatment of 12 Weeks

Figure 4. Profiles of Free Cl^- (Left) and Free TBA^+ (Right) concentrations (mM) and pH Levels (Middle) after the 3 A/m^2, 500 mM TBA-B Treatment, As a Function of Time

As an organic corrosion inhibitor, TBA-B is expected to mitigate the corrosion of steel by forming an adsorbed film onto the metallic substrate and thus acting as a barrier to limit the access of Cl^- and oxygen to the steel surface. A TBA^+ concentration as low as 5 mM on steel can effectively inhibit the corrosion of steel in a typical chloride-contaminated concrete or mortar (3.0 wt.% NaCl and pH=13) [27]. The inhibition function of TBA^+ generally increases with its concentration, and a concentration above 10 mM can be expected to form a reliable protective film on the steel surface.

In this context, a good evaluation of the electrochemical treatment (e.g., coupled ECE and EICI) of salt-contaminated mortar requires an accurate prediction of the relative concentration of Cl^-, OH^- and TBA^+ ions in the vicinity of rebar surface. First of all, the concentrations of Cl^-, OH^- and TBA^+ ions were predicted at three levels of current density (1 A/m^2, 3 A/m^2 and 5 A/m^2) for each of the four treatment duration: 1 week, 4 weeks, 8 weeks and 12 weeks, respectively. Considering that the diffusion coefficient of TBA^+ is apparently lower than those of Cl^- and OH^- ions, two concentration levels of TBA^+ (200 mM and 500 mM) were also evaluated to examine the effect of initial inhibitor concentration on the post-treatment distribution of ionic species. As such, a variety of electrochemical treatments were examined by the FEM model. Some results of FEM analyses are presented in Figure 2 and Figure 3.

4. DISCUSSION

4.1. Effect of current density and treatment time on ion distribution profiles after ECE

Figure 2 presents the concentration profiles of free Cl^- values in the mortar after the 8-week ECE treatment under three current density levels, 1 A/m^2, 3 A/m^2 and 5 A/m^2, based on the FEM model predictions. The non-uniform, nonlinear Cl^- concentration profiles clearly illustrate the results of ECE in removing Cl^- ions out of the repair mortar and the important effect of electrode location on

the treatment efficiency. The ECE treatment was not effective in decontaminating the zone behind the rebar, which is consistent with previous modeling studies [18, 49] and highlights the need for different electrode configurations [18,50,51] to enhance the chloride removal from severely contaminated mortars.

The modeling results suggest that the magnitude of current density has a significant effect on removing chloride out of the mortar and increasing the pH of the pore solution near the rebar. At 1 A/m^2, the 8-week ECE treatment decreased the free Cl^- concentration in the vicinity of the rebar surface by 44% (from 513 mM to 287 mM). At 3 A/m^2 and 5 A/m^2, the 8-week ECE treatment decreased the free Cl^- concentration in the vicinity of the rebar surface to 136 mM and 35 mM, i.e., by 74% and 93%, respectively. While the Cl^- removal in other zones of the repair mortar was not as high as that near the rebar, these results still confirm that the amount of chloride removed by ECE increases with the externally applied current density [18, 48]. The model also confirms that higher current density induced more pH increase near the steel rebar, as more hydroxyl ions were produced at the rebar surface and gradually migrated away from the rebar [18, 49]. While not presented in Figure 2, the modeling results also confirm that more $Na^+$and K^+ were transported into the zone close to the steel rebar as a result of increasing current density [49, 52]. All these changes in the ionic distribution in the repair mortar were induced by the ECE treatment, and they are likely responsible for the benefits of ECE in improving the compressive strength of mortar and reducing the corrosion rate of steel rebar reported elsewhere [35]. It is cautioned that when the underlying mortar or concrete contains reactive aggregates susceptible to alkali aggregate reactions (AARs), such electrochemical treatment should be avoided considering the highly alkaline environment they would produce [53].

The FEM model also predicted the concentration profiles of free Cl^- in the mortar after the 1 A/m^2 ECE treatment as a function of treatment time. The predictions confirm that the treatment time can have a significant effect on removing chloride out of the mortar and increasing the pH of the pore solution near the rebar [48, 49, 52]. The 1 A/m^2 ECE treatment decreased the free Cl^- concentration in the vicinity of the rebar surface from 513 mM to 341 mM, 337 mM, 287 mM, and 286 mM, i.e., by 33%, 34%, 44%, and 44%, respectively, as a function of time. These results also suggest that extending the treatment time under some scenarios (e.g., after one week of 1 A/m^2 treatment) may not be a productive way to improve chloride removal by ECE [48].

4.2. Effect of current density, treatment time, and initial inhibitor concentration on ion distribution profiles after coupled ECE and EICI

Figure 3 presents the concentration profiles of free Cl^- and TBA^+ and pH values in the mortar after the 12-week, 500 mM TBA-B treatment under three current density levels, 1 A/m^2, 3 A/m^2 and 5 A/m^2, based on the FEM model predictions. The non-uniform, nonlinear Cl^- concentration profiles clearly illustrate the results of ECE+EICI in removing Cl^- ions out of the repair mortar and the important effect of cathode location on the treatment efficiency. Similar to ECE, the ECE+EICI treatment was not effective in decontaminating the zone behind the rebar, which highlights the need for different electrode configurations for enhanced chloride removal. Note that the model might have slightly overestimated the alkalinity increases in the vicinity of the steel rebar, since it does not

incorporate the possible buffering effects by calcium hydroxide precipitation [54]. This study has predicted that with a high current density of 5A/m^2 (of steel surface) it takes quite a long period (12 weeks) for a significant amount of the inhibitor TBA-B to penetrate about 35 mm into the repair mortar (Figure 3c).

The modeling results suggest that the magnitude of current density has a significant effect on removing chloride out of the mortar and increasing the pH of the pore solution near the rebar. At 1 A/m^2, the 12-week ECE+EICI treatment decreased the free Cl^- concentration in the vicinity of the rebar surface by 25% (from 513 mM to 385 mM). At 3 A/m^2 and 5 A/m^2, the 12-week ECE+EICI treatment decreased the free Cl^- concentration in the vicinity of the rebar surface to 180 mM and 128 mM, i.e., by 65% and 75%, respectively. Contrasting these numbers with those under the ECE treatment, one can conclude that the injection of the corrosion inhibitor significantly slowed down the removal of chloride by the same galvanostatic treatments. The model predictions also suggest that higher current density induced more pH increase near the steel rebar and more injection of the inhibitor TBA^+ ions into the repair mortar. The benefits of increasing the current density to TBA^+ ion injection were less significant than chloride removal. The penetration depths of the organic corrosion inhibitor was similar [55] or less than those under some other ECE+EICI modeling [53] or experimental studies [54, 56], depending on the specific chemistry of the inhibitor and the microstructure and chemistry of the cementitious materials. The modeling results also confirm that more $Na^+$and K^+ were transported into the zone close to the steel rebar as a result of increasing current density. All these changes in the ionic distribution in the repair mortar were induced by the ECE+EICI treatment and were responsible for the observed benefits of such treatment in reducing the corrosion rate of the steel rebar [36].

Figure 4 presents the concentration profiles of free Cl^- and TBA^+ and pH values in the mortar after the 3 A/m^2, 500 mM TBA-B treatment as a function of treatment time. The results confirm that the treatment time can have a significant effect on removing chloride out of the mortar and increasing the pH of the pore solution near the rebar. The 3 A/m^2 ECE+EICI treatment decreased the free Cl^- concentration in the vicinity of the rebar surface from 513 mM to 334 mM, 282 mM, 231 mM, and 180 mM, i.e., by 35%, 45%, 55%, and 65%, respectively, as a function of time. After one week of 3 A/m^2 treatment, however, extending the treatment time did not serve as a productive way to improve TBA^+ injection by the electric field.

To examine the effect of initial inhibitor concentration on ion distribution profiles after coupled ECE and EICI, the FEM model also predicted the concentration profiles of free Cl^- and TBA^+ and pH values in the mortar after two scenarios of ECE+EICI treatments using three initial TBA-B concentrations. After the 1 A/m^2, 8-week treatment, the concentration of chloride near the rebar surface dropped by 44%, 25% and 25%, from 513 mM to 287 mM, 385 mM, and 385 mM, with an initial TBA-B concentration of 0, 200 mM, and 500 mM, respectively. After the 5 A/m^2, 12-week treatment, the concentration of chloride near the rebar surface dropped by 93%, 75% and 75%, from 513 mM to 34 mM, 128 mM, and 128 mM, with an initial TBA-B concentration of 0, 200 mM, and 500 mM, respectively. In both scenarios, the model predicted the negative effect of inhibitor injection on the efficiency of chloride removal by the galvanostatic treatments. As such, the selection of a better inhibitor or a better anolyte (e.g., saturated lime) is desirable to ensure sufficient chloride removal and inhibitor injection after an ECE+EICI treatment of reasonable duration and moderate current density.

In both scenarios, increasing the initial inhibitor concentration from 200 mM to 500 mM exhibited negligible effects on chloride removal, alkalinity increase, or inhibitor penetration.

According to the model predictions (shown in Figures 2 to 4), Cl^- and TBA^+ both feature a non-uniform concentration distribution near the rebar surface as a result of the electrochemical treatments, whereas hydroxyl ions around the rebar surface induce pH values close to 13.9. The simultaneous application of EICI with ECE is expected to help extend the effectiveness of the ECE treatment by providing TBA^+ ions to balance the potential attack of residual chloride ions to the rebar surface. After the electrochemical treatment, a polymer-based sealer can be placed on the exposed surface of the repair mortar. This serves to minimize any possible ingress of external chlorides, water, and other detrimental species and thus preserve the effectiveness of electrochemical rehabilitation [57].

5. CONCLUDING REMARKS

This work employs a two-dimensional FEM model developed to study the non-stationary transport behavior of ionic species under an external electric field, using a salt-contaminated and water-saturated repair mortar as case study. The apparent diffusion coefficients and Langmuir isotherm parameters of major species, i.e., the inhibitor TBA-B and chloride were experimentally determined. Starting from the equation of mass balance, the 2D model incorporates the mechanisms of natural diffusion and electromigration, and considers the important features of ionic transport in mortar such as integration of the multiple species and the chloride and inhibitor binding with hydration products. In this study, the mortar was treated as the bulk material and the potential interference of mortar/concrete interface to the model's boundary condition was not considered.

Based on the numerical results predicted by the FEM model, both the ECE alone and the ECE+EICI treatment were effective in decontaminating the zone in front of the rebar. In both techniques, the magnitude of current density has a significant effect on removing chloride out of the mortar and increasing the pH of the pore solution near the rebar. The injection of the corrosion inhibitor significantly slowed down the removal of chloride by the same galvanostatic treatments. Increasing the initial inhibitor concentration from 200 mM to 500 mM exhibited negligible effects on chloride removal, alkalinity increase, or inhibitor penetration. All the changes in the ionic distribution in the repair mortar were generally beneficial in reducing the corrosion risk of the steel rebar and thus extending the service life of the repair in chloride environments.

This study has predicted that with a high current density of 5 A/m^2 (of steel surface) it takes quite a long period (12 weeks) for a significant amount of the inhibitor TBA-B to penetrate about 35 mm into the repair mortar (Figure 3c). It is known that further increasing the current density would undermine the microstructure of the mortar [28]. As such, there is the urgent need to identify a corrosion inhibitor with higher diffusion coefficient [29] or to reduce the Na^+ concentration in the anolyte [20].

COMPLIANCE WITH ETHICAL STANDARDS
This study was funded by the National Natural Science Foundation of China (Grant number 51278390), the Hubei Provincial Department of Transportation Research Program (Project number 2016-600-1-10), and the Hubei Provincial Department of Construction Research Program (Project number EJB-2016-347-1-13). The authors declare that they have no conflict of interest.

References

1. L. Basheer, J. Kropp, and D.J. Cleland, *Constr. Build., Mater.*, 15 (2001) 93.
2. Y. Liu, and X. Shi, *J. Mater. Civ. Engng.*, 24 (2011) 381.
3. X. Shi, L. Fay, M.M. Peterson, and Z. Yang, *Mater. Struct.* 43 (2010) 933.
4. V.G. Papadakis, C.G. Vayenas, and M.N. Fardis, *ACI Mater. J.*; 88 (1991) 363.
5. A.V. Saetta, B.A. Schrefler, and R.V. Vitaliani, *Cem. Concr. Compos.*, 23 (1993) 761.
6. B. Tian, and M.D. Cohen, *Cem. Concr. Res.* 30 (2000) 117.
7. A. Neville, *Cem. Concr. Res.* 34 (2004) 1275.
8. X. Shi, N. Xie, K. Fortune, and J. Gong, *Constr. Build. Mater.* 30 (2012) 125.
9. C. Alonso, C. Andrade, M. Castellote, and P. Castro, *Cem. Concr. Res.* 30 (2000) 1047.
10. X. Shi, T.A. Nguyen, P. Kumar, and Y. Liu, *Anti-Corros. Meth. Mater.* 58 (2011) 179.
11. H. Yu, X. Shi, W.H. Hartt, and B. Lu, *Cem. Concr. Res.* 40 (2010) 1507.
12. G. Batis, A. Routoulas, and E. Rakanta, *Cem. Concr. Compos.*, 25 (2003) 109.
13. X. Shi, Z. Yang, T.A. Nguyen, Z. Suo, R. Avci, and S. Song, *Sci. China Ser. E: Technol. Sci.* 52 (2009) 52.
14. J. Bennett, T.J. Schue, K.C. Clear, D.L. Lankard, W.H. Hartt, and W.J. Swiat, Electrochemical Chloride Removal and Protection of Concrete Bridge Components: Laboratory Studies. Report # SHRP S-657, Strategic Highway Research Program, Washington, D.C., National Research Council. 1993.
15. J.K. Bennett, F. Fong, and T.J. Schue, Electrochemical Chloride Removal and Protection of Concrete Bridge Components: Field Trials. Report # SHRP S-669, Strategic Highway Research Program, Washington, D.C., National Research Council. 1993.
16. W. Yao, and Z. Zhao, *Sci. China Technol. Sci.* 53 (2010) 1466.
17. G. Fajardo, and A.G. Escadeillas, *Corros. Sci.* 48 (2006) 110.
18. Y. Liu, and X. Shi, *Constr. Build. Mater.* 27 (2012) 450.
19. W. Yodsudjai, and W. Saelim, *J. Mater. Civ. Engng.* 26 (2014), doi: 10.1061/(ASCE)MT.1943-5533.0000777.
20. R.B. Polder, R. Walker, and C.L. Page, In: *Strategic Highway Research Program (SHRP) and Traffic Safety on Two Continents, Proceedings of the Conference* (No. VTI 1A, Part 5), 1994.
21. A. Cañón, P. Garcés, M.A. Climent, J. Carmona, and E. Zornoza, *Corros. Sci.* 77 (2013) 128.
22. J.A. González, A. Cobo, M.N. González, and E. Otero, *Mater. Corros.* 51 (2000) 97.
23. E. Redaelli, M. Carsana, M. Gastaldi, F. Lollini, and L. Bertolini, *Corros. Rev.* 29 (2011) 179.
24. D. Whitmore, and S. Abbott, In: *Proceedings of the 11th International Conference on Alkali-Aggregate Reaction (ICAAR)*. Ed. M.A. Bérubé, et al. Quebec City, Canada. June 11-16, 2000; pp. 1089-1098.
25. J.-S. Ryu, and N. Otsuki, *J. Appl. Electrochem.* 32 (2002) 635.
26. S. Sawada, and C.L. Page, *Corros. Sci.* 47 (2005) 2063.
27. T. Pan, T.A. Nguyen, and X. Shi, *Transport. Res. Rec.* 2044 (2008) 51.
28. Y. Liu, and X. Shi, *Corros. Rev.* 27 (2009) 53.
29. M. Sánchez, and M.C. Alonso, *Constr. Build. Mater.* 25 (2011) 873.
30. S. Jorge, D. Dias-da-Costa, and E.N.B.S. Júlio, *Engng. Struct.* 36 (2012) 372.
31. N.R. Buenfeld, G.K. Glass, A.M. Hassanein, and J.Z. Zhang, *J. Mater. Civ. Engng.* 10 (1998) 220.
32. X. Shi, Z. Yang, Y. Liu, and D. Cross, *Constr. Build. Mater.* 25 (2011) 3245.

33. Z. Yang, X. Shi, A.T. Creighton, and M.M. Peterson, *Constr. Build. Mater.* 23 (2009) 2283.
34. X. Lu, C. Li, and H. Zhang, *Cem. Concr. Res.* 32 (2002) 323.
35. T.H. Nguyen, T.A. Nguyen, V.K. Le, H. Thai, X. Shi, and T.H. Nguyen, *Anti-Corros. Meth. Mater.* 63 (2016) 377.
36. T.H. Ngyuen, T.A. Nguyen, T.V. Nguyen, V.K. Le, T.M.T. Dinh, H. Thai, and X. Shi, *Intl. JJJ. Corros.* (2015) Article ID 862623, 10 pages, doi:10.1155/2015/862623.
37. E. Samson, J. Marchanad, and K.A. Snyder, *Mater. Struct.* 36 (2003) 156.
38. Florida Department of Transportation. Florida Method of Test for Determining Low-Levels of Chloride in Concrete and Raw Materials. FM-5-516, 2000.
39. X. Shi, L. Fay, K. Fortune, R. Smithlin, M. Johnson, M.M. Peterson, and A. Creighton, *Can. J. Civ. Engng.* 39 (2012) 117.
40. B.A. Finlayson, and L.E. Scriven, *ASME Appl. Mech. Rev.* 19 (1966) 735.
41. M.F.N. Mohsen, *Appl. Math. Model.* 6 (1982) 165.
42. S.Y. Chang, *J. Chin. Inst. Engr.* 27 (2004) 663.
43. L.Y. Li, and C.L. Page, *Comput. Mater. Sci.* 9 (1998) 303.
44. E. Samson, G. Lemaire, J. Marchand, and J.J. Beaudoin, *Comput. Mater. Sci.* 15 (1999) 285.
45. M. Castellote, C. Andrade, and C. Alonso, *Cem. Concr. Res.* 30 (2000) 1885.
46. C. Pereira, and L. Hegedus, In: *Proceedings of the 8th International Symposium on Chemical Reaction Engineering* 1984; 87: 427-438.
47. N. Moës, E. Béchet, and M. Tourbier, *Intl. J. Num. Meth. Engng.* 67 (2006) 1641.
48. R.G. Casten, and C.J. Holland, *J. Differ. Eqn.* 27 (1978) 266.
49. Y. Wang, L.Y. Li, and C.L. Page, *Comput. Mater. Sci.* 20 (2001) 196.
50. Q.F. Liu, J. Xia, D. Easterbrook, J. Yang, and L.Y. Li, *Constr. Build. Mater.* 70 (2014) 410.
51. C.C. Chang, W. Yeih, J.J. Chang, and R. Huang, *Constr. Build. Mater.* 68 (2014) 692.
52. A. Toumi, R. Francois, and O. Alvarado. *Cem. Concr. Res.* 37 (2007) 54.
53. P.F.G. Banfill, In: *Concrete Solutions* by M.G. Grantham, I. Papayianni, and K. Sideris (Eds), 2016, 113-119.
54. J. Kubo, S. Sawada, C.L. Page, and M.M. Page, *Corros. Sci.* 49 (2007) 1205.
55. C. Xu, W.L. Jin, H.L. Wang, H.T. Wu, N. Huang, Z.Y. Li, and J.H. Mao, *Constr. Build. Mater.* 115 (2016) 602.
56. F.L. Fei, J. Hu, Q.J. Yu, J.X. Wei, and Y.B. Nong, *Mater. Corros.* 66 (2015) 1039.
57. Y. Dang, N. Xie, A. Kessel, E. McVey, A. Pace, and X. Shi, *Construction and Building Materials*, 55 (2014) 128.